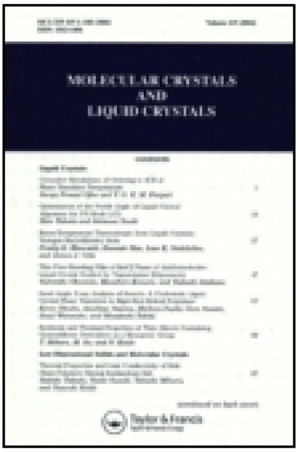

Molecular Crystals and Liquid Crystals Science and Technology. Section A. Molecular Crystals and Liquid Crystals

Publication details, including instructions for authors and subscription information:
http://www.tandfonline.com/loi/gmcl19

Modelling of Photoelectrical Properties of Metal/Organic Solid/Metal Systems

Ryszard Signerski [a] & Jankalinowski [b] [c]

[a] Department of Molecular Physics, Technical University of Gda[ngrave]sk, 80-952, Gda[ngrave]sk, Poland

[b] Istituto di Fotochimica e Radiazioni d'Alta Energia, CNR, 40-126, Bologna, Italy

[c] Department of Molecular Physics, Technical University of Gda[ngrave]sk, 80-952, Gda[ngrave]sk, Poland

Version of record first published: 24 Sep 2006.

To cite this article: Ryszard Signerski & Jankalinowski (1993): Modelling of Photoelectrical Properties of Metal/Organic Solid/Metal Systems, Molecular Crystals and Liquid Crystals Science and Technology. Section A. Molecular Crystals and Liquid Crystals, 228:1, 213-219

To link to this article: http://dx.doi.org/10.1080/10587259308032162

Mol. Cryst. Liq. Cryst. 1993, Vol. 228, pp. 213–219
Reprints available directly from the publisher
Photocopying permitted by license only

Printed in the United States of America

MODELLING OF PHOTOELECTRICAL PROPERTIES OF METAL/ORGANIC SOLID/METAL SYSTEMS*

RYSZARD SIGNERSKI
Department of Molecular Physics, Technical University of Gdańsk,
80-952 Gdańsk, Poland

JAN KALINOWSKI**
Istituto di Fotochimica e Radiazioni d'Alta Energia, CNR, 40-126 Bologna, Italy

Abstract A numerical treatment of injection photoconduction and photovoltaic characteristics of Metal/Organic Solid/Metal (M/OS/M) systems is proposed, accounting for bulk generation of electron-hole pairs by singlet exciton dissociation on neutral generation centres distributed exponentially throughout the sample. Examples of photocurrent-voltage and photovoltaic current versus absorption coefficient and flux of the active light characteristics are presented and discussed in relation to dark generated carriers and spatial distribution of the electric field in the sandwich-type samples. They agree qualitatively with those observed in typical M/OS/M systems, where charge generation is due to contact and bulk operation of singlet excitons (e.g. anthracene or phthalocyanine-like sandwich cells).

INTRODUCTION

Photoelectrical properties of Metal/Organic Solid/Metal (M/OS/M) systems are of interest by virtue of their applications as well as their importance in understanding of physically fundamental electronic processes in organic solids.[1-3] A huge number and variety of organic materials lead to a differentiation in photogeneration mechanisms of charge carriers in such systems and unable universal description of their photoelectrical properties.

A simple treatment of unipolar injection photoconduction and photovoltaic characteristics for organic solids when photogeneration of electrons and holes within the bulk can be neglected has been recently reinvestigated by us and applied to M/Tetracene/M sandwich-type system.[4] In the case where bulk generation is operative, there exists no simple treatment of photoelectrical phenomena at present. In this work an attempt has been made to numerical simulate some photoelectrical characteristics of M/OS/M systems, accounting for bulk generation of electrons and holes by singlet exciton dissociation on unspecified neutral generation centres distributed exponentially throughout the sample.

---

* The work supported in part by the Polish State Research Council (KBN) under project nr. 204599101 for the period 1992-1994.

** On leave from Department of Molecular Physics, Technical University of Gdańsk, 80-952 Gdańsk, Poland.

BASIC ASSUMPTIONS

M/OS/M systems investigated are illustrated in Figure 1.

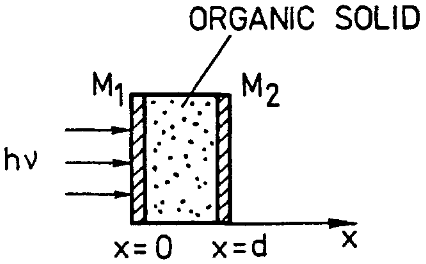

FIGURE 1 Schematic diagram of the M/OS/M systems investigated. M_1, M_2 - semitransparent metal electrodes deposited onto the organic material layer of thickness d. Photoelectrical phenomena are induced by light (hν) entering the system by one of the semitransparent metallic electrodes.

Within the framework of the present discussion we shall be concerned with the following physical conditions.

a. Carrier generation involves a highly absorbed light, excluding multi-photon processes (absorption coefficient κ and photon flux I_o).

b. The photo-carriers are produced solely via singlet excitons (S- singlet exciton concentration, k_s– their monomolecular decay constant, and γ_{SM} - second order rate constant of the exciton-neutral generation center interaction).

c. The free carrier concentration (p) is a result of the following processes:
   - thermal and singlet exciton injection from the sample interfaces ($x = 0$, $x = d$),
   - singlet exciton dissociation on neutral generation centres (the effective rate constant for both interface injection and dissociation near by the surface given by α),
   - thermal detrapping of the charge trapped in the sample (p_t – concentration of the trapped carriers, γ_p - second order trapping rate constant),
   - thermal ionization of neutral generation centres (M_n – concentration and k_M – ionization rate constant of the centres).

d. Single positive carriers (holes) are responsible for the charge transport; negative carriers are localized, influencing internal electric field in the sample (μ - mobility of holes, γ_{pM} - second order rate constant for the recombination free charge carriers (p) - ionized centres (M^-)) .

e. A discrete set of traps plays a dominant rolė in determining the ratio of the free to trapped carrier concentration ratio (E_t - depth and H - concentration of traps).

SET OF EQUATIONS

A complete set of equations describing photoelectrical behaviour of the systems defined in the previous section must contain kinetic equations for singlet excitons (S)

$$\kappa I_0 e^{-\kappa x} - k_S S - \gamma_{SM} S M_n = 0 , \qquad (1)$$

for trapped (p_t)

$$\nu \exp(-E_t/kT)\, p_t - \gamma_p\, p(H - p_t) = 0 \qquad (2)$$

and free (p) charge carriers

$$k_M M_n + \gamma_{SM} S M_n = \gamma_{pM}\, p M^- , \qquad (3)$$

and the balance equation for the generation centres

$$M = M_n + M^- \; . \qquad (4)$$

The remaining equations relating unipolar (hole) current j, free charge carrier density p, and the internal electric field F for one-dimensional systems are

$$j = e\mu p F - \mu k T \frac{dp}{dx} , \qquad (5)$$

where the carrier diffusion coefficient (D) is related to its mobility (μ) by the Einstein equation $D = \mu kT/e$, and the electric field obeys Poisson's equation

$$\frac{dF}{dx} = \frac{e}{\epsilon} (p + P_t - M^-) , \qquad (6)$$

where ϵ is the absolute dielectric constant of the organic solid.

Combining equations (5) and (6) leads to a differential equation for p:

$$\frac{d^2p}{dx^2} + \frac{1}{p}\left(\frac{j}{\mu kT} + \frac{dp}{dx}\right)\frac{dp}{dx} - \frac{e^2 p}{\epsilon kT} (p + P_t - M^-) = 0 \; . \qquad (7)$$

A numerical solution of Eq. (7) requires the boundary conditions for $p\,(x=0) = p_0$ and $p(x=d) = p_d$ (see Ref. 5).

Due to the strongly absorbed light only at the illuminated front electrode

$$p_0 = p_0^{th} + \alpha \kappa I_0 . \qquad (8)$$

The free carrier concentration at the exit (x = d) electrode equals the carrier concentration produced solely by thermal (th) injection of holes and dissociation of generation centres

$$p_d = p_d^{th} . \tag{9}$$

Upon taking into account these boundary conditions, one can rewrite Eq. (5) as

$$U = \frac{j}{e\mu} \int_0^d \frac{dx}{p} - \frac{kT}{e} \ln \left(\frac{p_0 \, p_d^{th}}{p_d \, p_0^{th}} \right) , \tag{10}$$

where U is the external voltage applied to the system.

The numerical solution of Eqs. (1) - (4), and (7) and (10) yields a series of graphical representations of the current (j) as a function of voltage (U), light intensity (I_0) and absorption coefficient (κ) of the active light. The spatial distribution of the field F(x) can be calculated from Eq. (5) or (6).

EXAMPLES OF CALCULATIONS

Figures 2, 3 and 4 show the current as a function of U, κ and I_0 for different system parameters and boundary conditions.

The following numbers have been used in all of the calculations:

$k_s = 10^9\ s^{-1}$, the frequency factor $\nu = 10^{12}\ s^{-1}$, the effective density of states $N_{eff} = \nu/\gamma_p = 10^{21}\ cm^{-3}$, $\mu = 0.4\ cm^2/Vs$, $k_M = 1\ s^{-1}$ (unless other value specified in figure captions), $\gamma_{SM} = 10^{-7} cm^3 s^{-1}$, $\gamma_{pM} = 10^{-8}\ cm^3\ s^{-1}$, $\alpha = 10^{-7} s$, $E_t = (0.4 - 0.7) eV$, $H = (10^{15} - 10^{18})\ cm^{-3}$ and $p^{th} = (10^6 - 10^{10})\ cm^{-3}$.

In addition, an exponential distribution of the neutral generation centres in space has been assumed according to

$$M(x) = M_0 \exp(-\beta x) + M_B \tag{11}$$

with $M_0 = 10^{17}\ cm^{-3}$, $M_B = 10^{12}\ cm^{-3}$ and $\beta = 10^2/d$.

The utility of this treatment can be tested in organic materials by a comparison with experimental results.

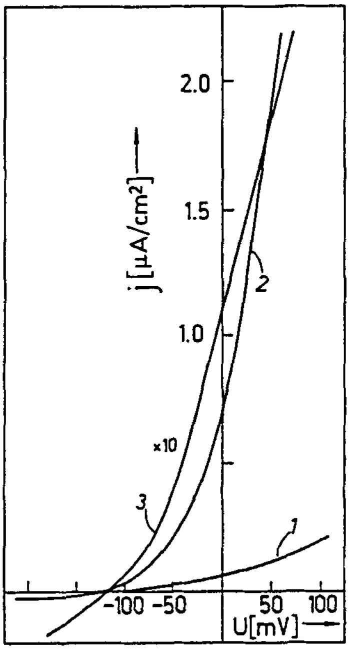

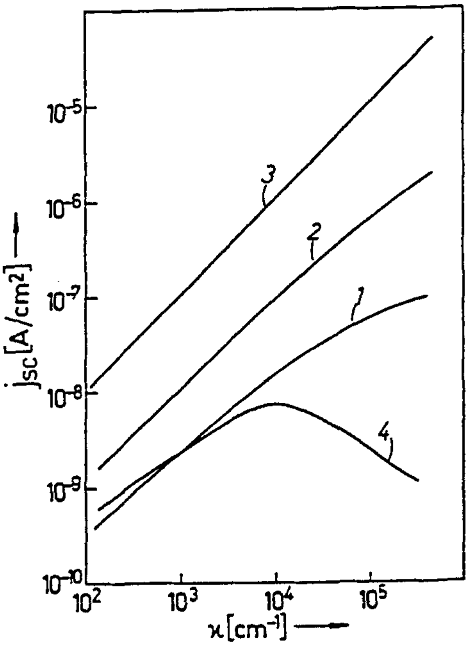

FIGURE 2 Calculated current-voltage plots for various injection and trapping conditions, and various sample thickness. d = 0.5 μm (curves 1 and 3), d = 2 μm (curve 2). Curves 1,2,3: $p_0^{th} = 10^9$ cm^{-3}, $E_t = 0.4$ eV; curves 1,2: $p_d^{th} = 10^8$ cm^{-3}, $H = 10^{18}$ cm^{-3}; curve 3: $p_d^{th} = 10^{10}$ cm^{-3}, $H = 10^{15}$ cm^{-3}. In all the cases $I_0 = 10^{13}$/cm^2 s and $\kappa = 10^5$ cm^{-1}.

FIGURE 3 Short-circuit current (j_{sc}) as a function of absorption coefficient at $I_0 = 10^{13}$/cm^{2}s. Curves 1,2,3 obtained at the conditions as in Figure 2. Curve 4: d = 2 μm, $p_0^{th} = 10^6$ cm^{-3}, $p_0^{th} = 10^{10}$ cm^{-3}, $E_t = 0.7$ eV, $H = 10^{16}$ cm^{-3}, $M_0 = 0$, $M_B = 10^{16}$ cm^{-3}, $k_M = 0$.

For instance, fill factor defined as

$$FF = \left| \frac{(jU)_{max}}{j_{SC} U_{OC}} \right| \qquad (jU < 0) \qquad (12)$$

can be calculated from the data of Figure 2. Its values for particular curves FF(1) = 0.16, FF(2) = 0.12 and FF(3) = 0.2 fall in the range of experimental data for organic materials.[6-8] Also, energy conversion factor

$$\eta_E = \frac{(jU)_{max}}{P_\lambda} \, 100\% , \qquad (13)$$

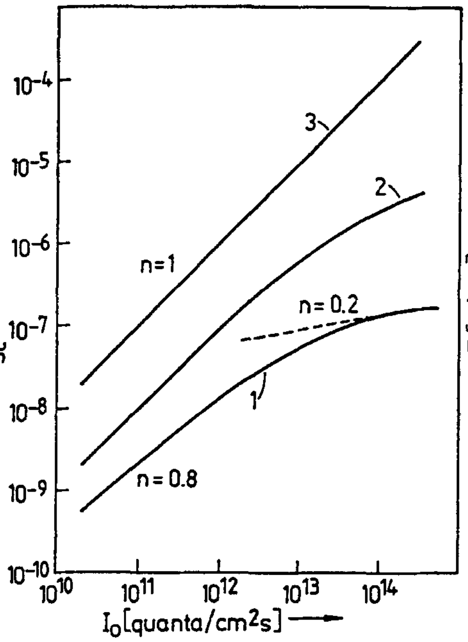

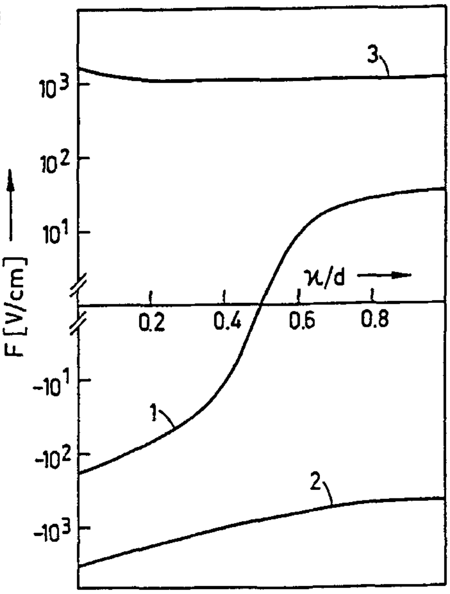

FIGURE 4 Several short-circuit current-light intensity dependences for $\kappa = 10^5$ cm^{-1}, under other conditions as specified for curves 1,2,3 in Figure 2.

FIGURE 5 The field distribution under short-circuit current flow in three different cases corresponding to curves 1,2,3 in Figure 2 with $I_0 = 10^{13}/\text{cm}^2\text{s}$ and $\kappa = 10^5\text{cm}^{-1}$

where P_λ is the radiation power, takes the values $\eta_E(1) = 0.03\%$, $\eta_E(2) = 0.3\%$ and $\eta_E(3) = 7\%$ with $\lambda =$ 600 nm, and corresponds well to experimental data of $\eta_E << 1\%$ and only in some particular cases approaching 1% (see Refs. 6-9).

It is noteworthy that the spectral behaviour of j_{sc} can be symbatic or anibatic with absorption, dependent on trapping conditions and range of κ (see Figure 3); the results corresponding to experimental observations.[4-8]

Light intensity dependence of j_{SC} can be approximated by a power function $j_{SC} \sim I_0^n$ with n changing from 1 to 0 for various material and experimental conditions (see Figure 4) as comes from experiment.[3-5,7]

The shape of the photovoltaic current (j_{SC}) characteristics reflects the field distribution inside the sample (see Figure 5), which, on the other hand, is a result of charge distribution, and, in particular, the ratio of charge concentration at the electrodes.

CONCLUSIONS

It has been shown that the recurrent features of photoelectrical properties observed with chemically different M/OS/M systems can be understood in terms of a model which is conceptionally simple yet unable to tackle analytically. Numerical solutions of the system of equations describing current flow are, however, a useful tool to determine how the combinations of physical assumptions, for instance, the type of electric contacts, and material parameters such as the energy and spatial distributions of carrier traps and carrier generation centres translate into macroscopic properties.

This conclusion is based on the fact that all observed photoelectrical features can consistently be explained in terms of the model while various analytical approximations lead to inconsistences. Presented examples of photocurrent-voltage and photovoltaic current versus absorption coefficient and flux of the active light characteristics agree qualitatively with those observed in typical M/OS/M systems, where charge carrier generation is due to contact and bulk operation of singlet excitons (e.g. anthracene- or phthalocyanine-like sandwich cells).

REFERENCES

1. K.C. Kao and W. Hwang, Electrical Transport in Solids, Pergamon Press, Oxford (1981).
2. M. Pope and C.E. Swenberg, Electrical Processes in Organic Crystals, Clarendon, Oxford (1982).
3. J. Simon and J.-J. André, Molecular Semiconductors, Springer-Verlag, Berlin (1985).
4. R. Signerski, J. Kalinowski, I. Koropecký and S. Nešpůrek, Thin Solid Films, 121, 175 (1984).
5. R. Signerski, Ph. D. Thesis, Technical University of Gdańsk, 1990 (in Polish).
6. V.Y. Merrit in Electrical Properties of Polymers (Edited by D.A. Seanor) ch. 4, Academic Press, New York (1982).
7. M. Martin, J.-J. André and J. Simon, Nouv.J.Chim., 5, 485 (1981).
8. G.A. Chamberlain, Solar Cells, 8, 47 (1983).
9. G. Horowitz, Adv. Mater., 2, 287 (1990).